RECENT PROGRESS ON NUCLEAR CHIRALITY IN COVARIANT DENSITY FUNCTIONAL THEORY*

Y.K. Wang, P.W. Zhao†

State Key Laboratory of Nuclear Physics and Technology, School of Physics
Peking University, Beijing 100871, China

(Received January 29, 2020)

Nuclear chirality is one of the hot topics in nuclear physics and has attracted great interests in the past decades. Studies on nuclear chirality in both experimental and theoretical sides have been carried out extensively. Among various theoretical investigations, the microscopic covariant density functional theory (CDFT) plays important roles. In this contribution, recent applications of the three-dimensional tilted axis cranking covariant density functional theory (3DTAC-CDFT) on nuclear chirality are reviewed. In particular, the multiple chirality in ^{106}Rh and the chiral conundrum in ^{106}Ag are discussed.

DOI:10.5506/APhysPolBSupp.13.567

1. Introduction

Chirality is a phenomenon with general interest in biology, chemistry, and physics. The chirality in atomic nuclei was first proposed by Frauendorf and Meng in 1997 [1]. It represents a novel dynamical collective mode of triaxial nuclei, where the angular momenta of valence protons, valence neutrons, and the core in the intrinsic frame can couple to each other and form either a left- or right-handed system. The arrangement of angular momenta in the left- and right-handed systems leads to the spontaneous chiral symmetry breaking. The restoration of chiral symmetry in the laboratory frame gives rise to a pair of nearly degenerate $\Delta I = 1$ sequences with the same parity, *i.e.*, chiral doublet bands [2]. So far, more than 60 chiral doublet candidates have been reported experimentally in the $A \sim 80$ [3, 4], 100 [5–9], 130 [10–16], and 190 [17, 18] mass regions of the nuclear chart, which indicates the robustness of nuclear chirality.

* Presented at the XXVI Nuclear Physics Workshop *Key problems of nuclear physics*, Kazimierz Dolny, Poland, September 24–29, 2019.

† Corresponding author: pwzhao@pku.edu.cn

In 2006, based on the adiabatic and configuration fixed constrained covariant density functional theory (CDFT), the existence of more than one pair of chiral doublets in one single nucleus, abbreviated as MχD, has been proposed [19]. The experimental evidences of MχD have been reported in nuclei ^{133}Ce [16], ^{103}Rh [20], ^{78}Br [4], and ^{136}Nd [21]; see data table [22] for details.

Theoretically, nuclear chirality has been extensively investigated by the triaxial particle-rotor model (PRM) [1, 23–26]. However, such investigations are all phenomenological and the contained parameters need to be determined by fitting the data in one way or another. The three-dimensional tilted axis cranking model provides a microscopic way to study the nuclear chirality [2] and it has been extended by combining with the shell correction method [27] or the Skyrme–Hartree–Fock mean field [28].

During the past decades, nuclear density functional theories (DFTs) have achieved great successes in describing many nuclear phenomena [29–32]. In particular, CDFT includes naturally the spin degrees of freedom and provides a self-consistent description of nuclear currents and time-odd fields, which plays important roles in describing the nuclear rotations [33–35]. Recently, the CDFT has been extended for investigating nuclear chirality with the tilted axis cranking approach [36], *i.e.*, 3DTAC-CDFT. The energy spectra and transition probabilities of the observed chiral bands in ^{106}Rh are well-reproduced and the chiral geometry along the bands is clearly shown by the orientation angles of the total angular momentum. Later on, the 3DTAC-CDFT has also been applied to solve the nuclear chiral conundrum with crossing twin bands in ^{106}Ag and a microscopic solution for the conundrum is provided [37].

In this contribution, the descriptions for nuclear chirality in ^{106}Rh and ^{106}Ag are presented and discussed in details.

2. Results and discussion

In Fig. 1, the rotational excitation energies, rotational frequencies, and $B(\mathrm{M1})/B(\mathrm{E2})$ ratios for the negative-parity chiral doublets observed in ^{106}Rh are depicted, in comparison with the results calculated by 3DTAC-CDFT with the PC-PK1 functional [38] based on the $\pi g_{9/2}^{-1} \otimes \nu h_{11/2}^{1}$ configuration. The numerical details of the 3DTAC-CDFT calculations can be found in Ref. [36]. Note that the energy splitting and the quantum tunneling between the left- and right-handed systems cannot be described on the present mean-field level and, therefore, only the band with lower excitation energies, *i.e.*, Band 1, can be reproduced. For the description of the partner band, one needs to go beyond the mean-field calculations by combining, for example, the methods of the random phase approximation [15] or the collective Hamiltonian [39] with the CDFT.

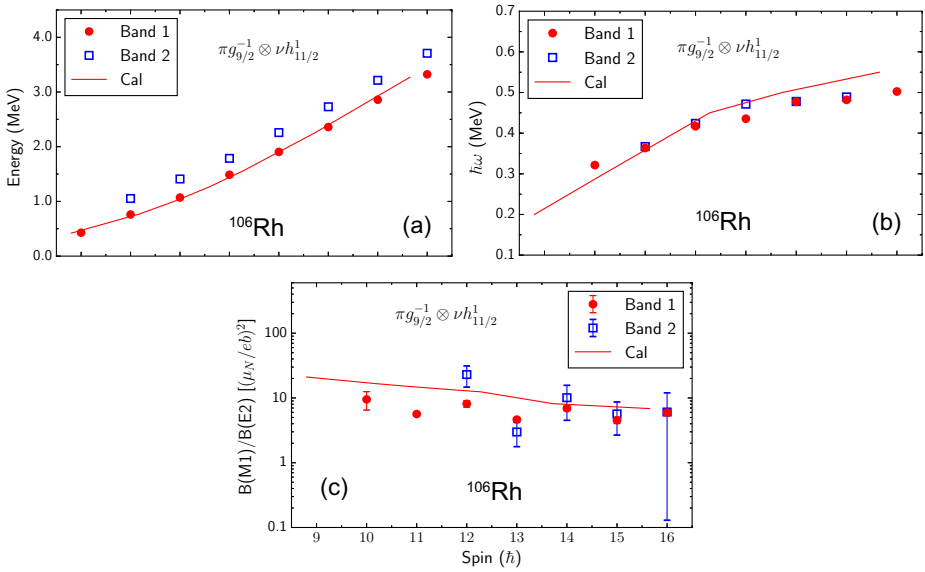

Fig. 1. Calculated rotational excitation energies (a), rotational frequencies (b), and $B(\mathrm{M1})/B(\mathrm{E2})$ ratios (c) for the $\pi g_{9/2}^{-1} \otimes \nu h_{11/2}^{1}$ configuration in ^{106}Rh, as a function of total angular momentum with the experimental data [40]. The excitation energies are renormalized to the ground state. Taken from Ref. [36].

As presented in Fig. 1 (b), the experimental rotational frequencies $\hbar\omega$ for the twin bands show very similar behaviors and are-well reproduced by the 3DTAC-CDFT calculations. In particular, the observed kink around $I = 12\hbar$, where the slope of the rotational frequencies as a function of spin changes abruptly, are also well-reproduced. As demonstrated in Ref. [36], the occurrence of this kink is connected with the change from the planar to the aplanar solutions, *i.e.*, chiral solutions, which can be clearly seen from the evolution of orientation angles of the total angular momentum (see Fig. 3 in Ref. [36] for details).

The calculated $B(\mathrm{M1})/B(\mathrm{E2})$ ratios also agree well with the experimental data, as shown in Fig. 1 (c). The calculated $B(\mathrm{M1})/B(\mathrm{E2})$ ratios decrease with the spin and present a kink at around $I = 12\hbar$. As discussed in Ref. [36], below the spin region of $I = 12\hbar$, the calculated $B(\mathrm{E2})$ values keep roughly unchanged due to the fact that the quadrupole deformation parameters (β, γ) stay almost constant along the bands. However, the $B(\mathrm{M1})$ values decrease smoothly with spin and thus, lead to the decreasing behavior of $B(\mathrm{M1})/B(\mathrm{E2})$ ratios. Above the $I = 12\hbar$ region, both $B(\mathrm{M1})$ and $B(\mathrm{E2})$ values go through a steep rise due to the change from the planar to the chiral solutions, but the ratios of $B(\mathrm{M1})$ and $B(\mathrm{E2})$ values still decrease with spin and exhibit a kink at around $I = 12\hbar$.

In Fig. 2, the calculated rotational excitation energies and the rotational frequencies $\hbar\omega$ for Bands 1 and 2 observed in ^{106}Ag as well as their comparison with the data [8] are depicted. As demonstrated in Ref. [37], the configurations for Bands 1 and 2 are assigned as $\pi g_{9/2} \otimes \nu h_{11/2}$ and $\pi g_{9/2} \otimes \nu h_{11/2}(gd)^2$ respectively. The calculated results can reproduce the data of Bands 1 and 2 very well. In particular, the energy differences of Bands 1 and 2 are also well-reproduced, which can be attributed to the inclusion of pairing correlations in the description of Band 1. Moreover, no configurations are found to be proper to describe Band 3 as mentioned in Ref. [37]. Due to the fact that the excitation energies and the quasiparticle alignments of Bands 2 and 3 are similar to each other [8], one can expect that Band 3 might be a chiral partner of Band 2. In fact, the Routhian curve of Band 2 as a function of azimuthal angle ϕ_ω grows very slowly [37], which indicates that chiral vibration between left- and right-handed systems should be substantial, and Bands 2 and 3 might be connected with chiral vibration.

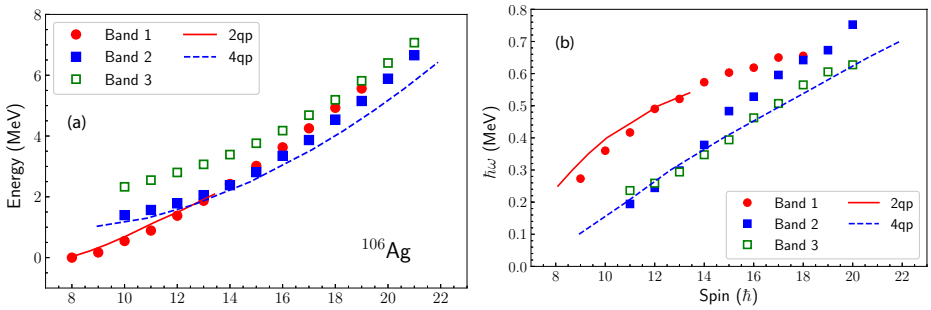

Fig. 2. Calculated rotational excitation energies (left) and rotational frequencies (right) based on the two- and four-quasiparticle configurations as a function of total angular momentum, in comparison with the experimental data [8]. The rotational excitation energies are renormalized to the bandhead. Taken from Ref. [37].

The calculated B(M1) and B(E2) values for Bands 1 and 2 based on the two- and four-quasiparticle configurations as well as their comparisons with the data are shown in Fig. 3. The calculated results reproduced the data very well and this further supports the configuration assignment for Bands 1 and 2. For both bands, the calculated B(E2) values keep roughly unchanged which is caused by the fact that the corresponding quadrupole deformation changes only slightly along the bands. The calculated B(M1) values, however, decrease smoothly with spin due to the gradual close of the proton and neutron angular momentum vectors.

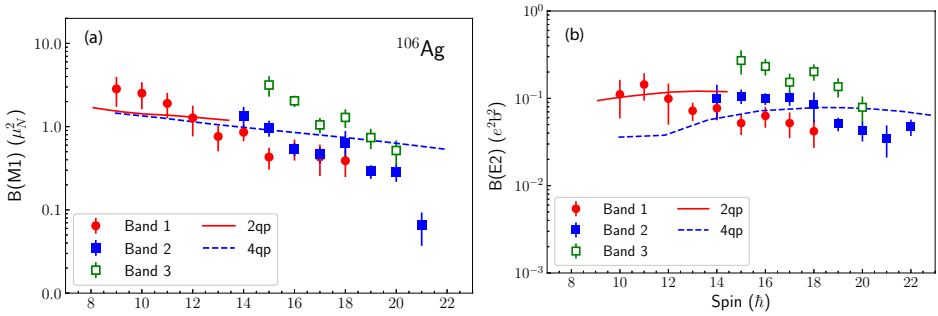

Fig. 3. Calculated B(M1) (left) and B(E2) (right) values with the two- and four-quasiparticle configurations as a function of the angular momentum, in comparison with the data [8]. Taken from Ref. [36].

3. Summary

In summary, the chirality in ^{106}Rh and the chiral conundrum in ^{106}Ag have been discussed with the recently developed framework of the three-dimensional tilted axis cranking covariant density functional theory. The experimental energy spectra, rotational frequencies, and the transition probabilities of nuclei ^{106}Rh and ^{106}Ag are well-reproduced. It supports the appearance of the chiral geometry in ^{106}Rh, and provides a microscopic solution for the chiral conundrum with crossing bands in ^{106}Ag.

We thank Q.B. Chen, S.Q. Zhang, and J. Meng for stimulating discussions and fruitful collaborations. This work was partly supported by the National Key R&D Program of China (contracts No. 2018YFA0404400 and No. 2017YFE0116700) and the National Natural Science Foundation of China (grants Nos. 11621131001, 11875075, 11935003, and 11975031).

REFERENCES

[1] S. Frauendorf, J. Meng, *Nucl. Phys. A* **617**, 131 (1997).
[2] S. Frauendorf, *Rev. Mod. Phys.* **73**, 463 (2001).
[3] S.Y. Wang *et al.*, *Phys. Lett. B* **703**, 40 (2011).
[4] C. Liu *et al.*, *Phys. Rev. Lett.* **116**, 112501 (2016).
[5] C. Vaman *et al.*, *Phys. Rev. Lett.* **92**, 032501 (2004).
[6] P. Joshi *et al.*, *Phys. Rev. Lett.* **116**, 102501 (2016).
[7] D. Tonev *et al.*, *Phys. Rev. Lett.* **112**, 052501 (2014).
[8] E.O. Lieder *et al.*, *Phys. Rev. Lett.* **112**, 202502 (2014).
[9] N. Rather *et al.*, *Phys. Rev. Lett.* **112**, 202503 (2014).

[10] K. Starosta *et al.*, *Phys. Rev. Lett.* **86**, 971 (2001).
[11] S. Zhu *et al.*, *Phys. Rev. Lett.* **91**, 132501 (2003).
[12] D. Tonev *et al.*, *Phys. Rev. Lett.* **96**, 052501 (2006).
[13] C.M. Petrache, G.B. Hagemann, I. Hamamoto, K. Starosta, *Phys. Rev. Lett.* **96**, 112502 (2006).
[14] E. Grodner *et al.*, *Phys. Rev. Lett.* **97**, 172501 (2006).
[15] S. Mukhopadhyay *et al.*, *Phys. Rev. Lett.* **99**, 172501 (2007).
[16] A.D. Ayangeakaa *et al.*, *Phys. Rev. Lett.* **110**, 172504 (2013).
[17] D.L. Balabanski *et al.*, *Phys. Rev. C* **70**, 044305 (2004).
[18] E.A. Lawrie *et al.*, *Phys. Rev. C* **78**, 021305 (2008).
[19] J. Meng, J. Peng, S.Q. Zhang, S.G. Zhou, *Phys. Rev. C* **73**, 037303 (2006).
[20] I. Kuti *et al.*, *Phys. Rev. Lett.* **113**, 032501 (2014).
[21] C.M. Petrache *et al.*, *Phys. Rev. C* **97**, 041304 (2018).
[22] B.W. Xiong, Y.Y. Wang, *At. Data Nucl. Data Tables* **125**, 193 (2019).
[23] J. Peng, J. Meng, S.Q. Zhang, *Phys. Rev. C* **68**, 044324 (2003).
[24] T. Koike, K. Starosta, I. Hamamoto, *Phys. Rev. Lett.* **93**, 172502 (2004).
[25] S.Q. Zhang, B. Qi, S.Y. Wang, J. Meng, *Phys. Rev. C* **75**, 044307 (2007).
[26] B. Qi *et al.*, *Phys. Lett. B* **675**, 175 (2009).
[27] V.I. Dimitrov, S. Frauendorf, F. Dönau, *Phys. Rev. Lett.* **84**, 5732 (2000).
[28] P. Olbratowski, J. Dobaczewski, J. Dudek, W. Płóciennik, *Phys. Rev. Lett.* **93**, 052501 (2004).
[29] P. Ring, *Prog. Part. Nucl. Phys.* **37**, 193 (1996).
[30] M. Bender, P.-H. Heenen, P.-G. Reinhard, *Rev. Mod. Phys.* **75**, 121 (2003).
[31] J. Meng *et al.*, *Prog. Part. Nucl. Phys.* **57**, 470 (2006).
[32] J. Meng (Ed.) «Relativistic Density Functional for Nuclear Structure», *World Scientific*, Singapore 2015.
[33] A.V. Afanasjev, P. Ring, *Phys. Rev. C* **62**, 031302 (2000).
[34] P.W. Zhao *et al.*, *Phys. Lett. B* **699**, 181 (2011).
[35] P.W. Zhao *et al.*, *Phys. Rev. Lett.* **107**, 122501 (2011).
[36] P.W. Zhao, *Phys. Lett. B* **773**, 1 (2017).
[37] P.W. Zhao, Y.K. Wang, Q.B. Chen, *Phys. Rev. C* **99**, 054319 (2019).
[38] P.W. Zhao, Z.P. Li, J.M. Yao, J. Meng, *Phys. Rev. C* **82**, 054319 (2010).
[39] Q.B. Chen *et al.*, *Phys. Rev. C* **87**, 024314 (2013).
[40] P. Joshi *et al.*, *Phys. Lett. B* **595**, 135 (2004).